A Bayesian Hierarchical Framework for Spatial Modeling of fMRI Data

Brian Caffo
Department of Biostatistics
Johns Hopkins University

MRI

- Nuclear magnetic resonance
  - Uniform magnetic field
  - Protons align in the direction of the magnetic field
  - Emitted RF pulse knocks protons out of alignment
  - Protons snap back into place emitting RF pulse
  - Emitted RF pulse differs by tissue type
  - Different pulse sequencing schemes yield images that highlight different anatomical structures

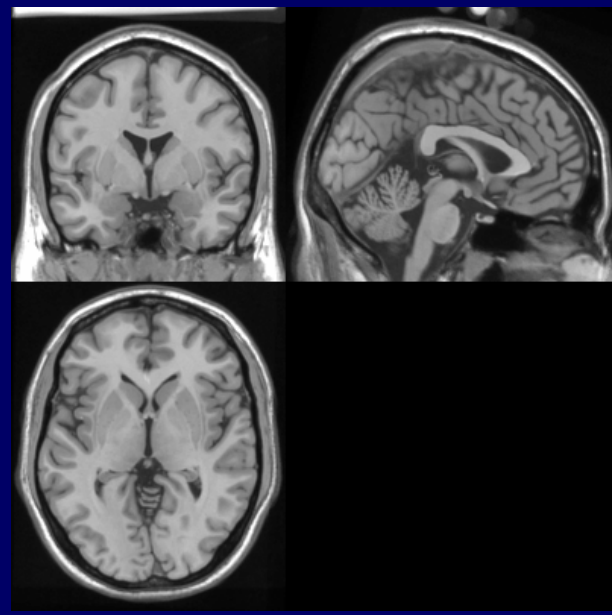

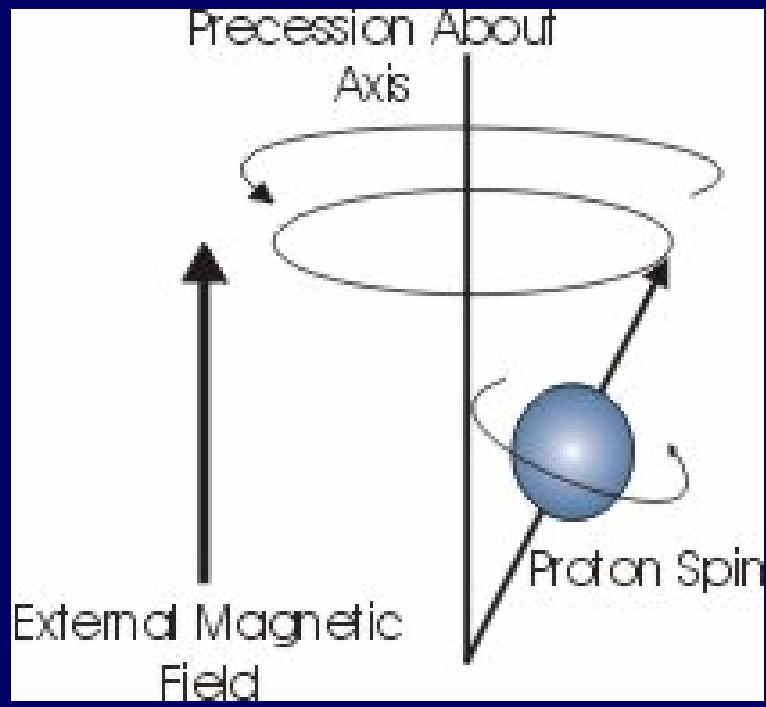

Functional Magnetic Resonance Imaging

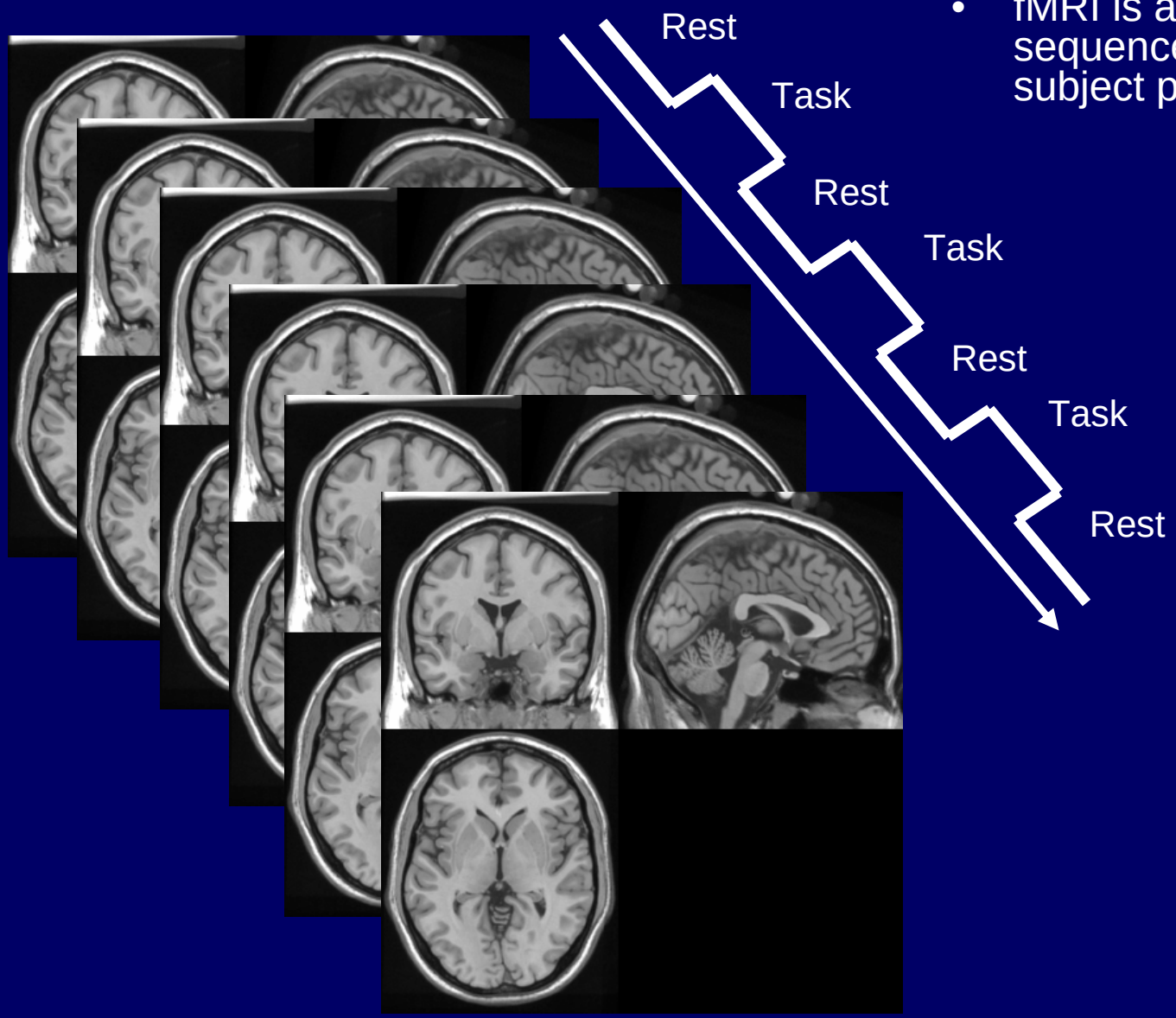

- fMRI is a technique for taking a sequence of MRIs while a subject performs a task

BOLD (blood oxygenation level dependent) Signal

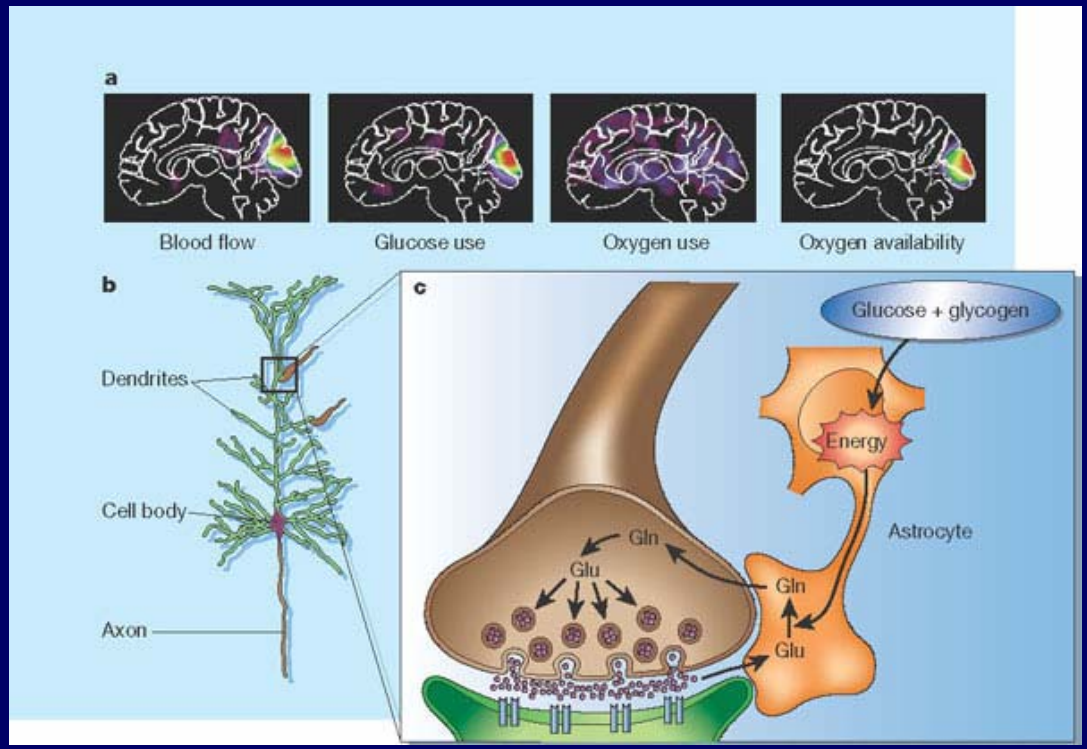

Marcus E. Raichle, Nature 412

Turner, Magnetic Resonance in Medicine 22

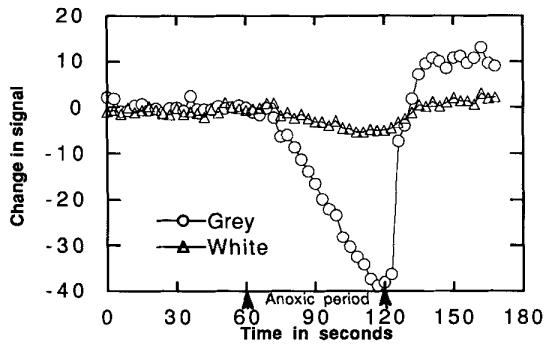

FIG. 4. Plot of the image difference (ROIs in gray and white matter) versus time, for the anoxia experiment. The maximum image intensity was 243. After anoxia commenced the signal for gray matter dropped steadily until oxygen was restored, at which time there was a sudden recovery and overshoot of image intensity. These changes were also seen, though smaller in amplitude, in white matter, reflecting the relative perfusion rates.

Idealized fMRI block design experiment

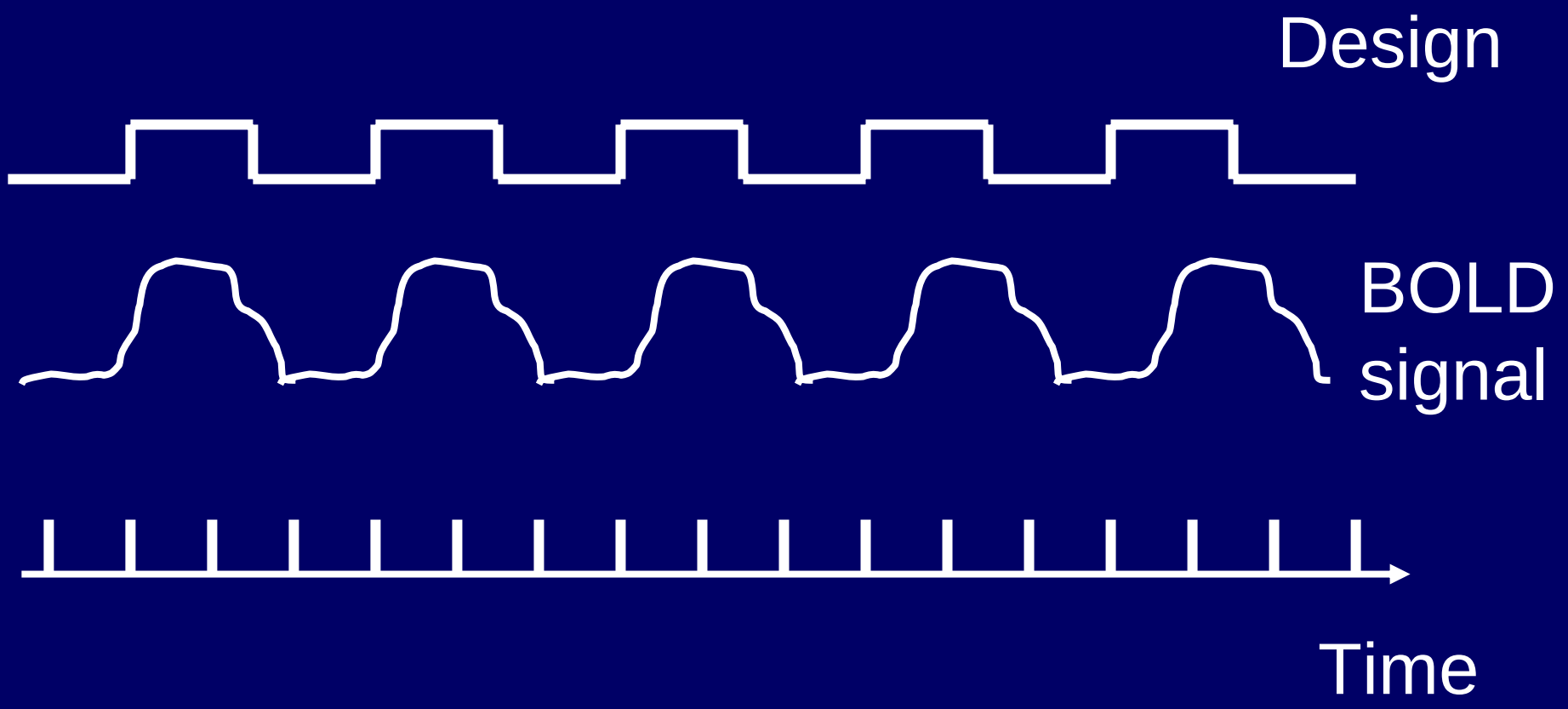

Hemodynamic response function

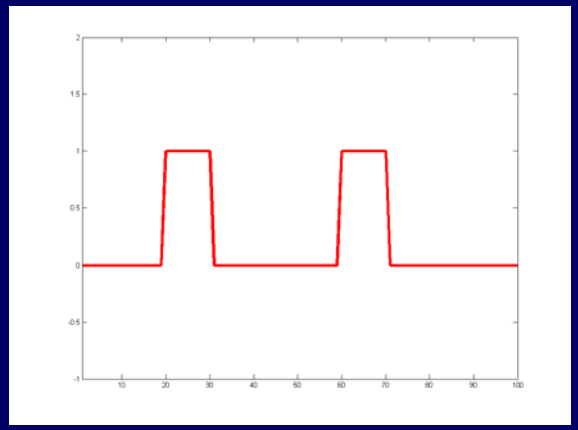

Boxcar design function

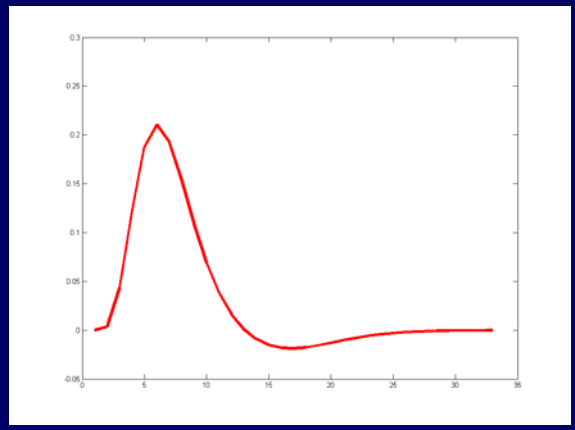

HRF

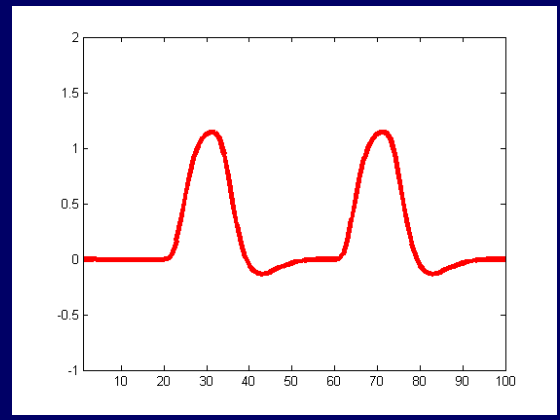

After convolution

- Physiologic delay from the onset of the task to the bold signals
- Small drop in blood oxygenation while oxygen is being replenished
- To account for this boxcar design function is convolved with a canonical hemodynamic response function

Example data

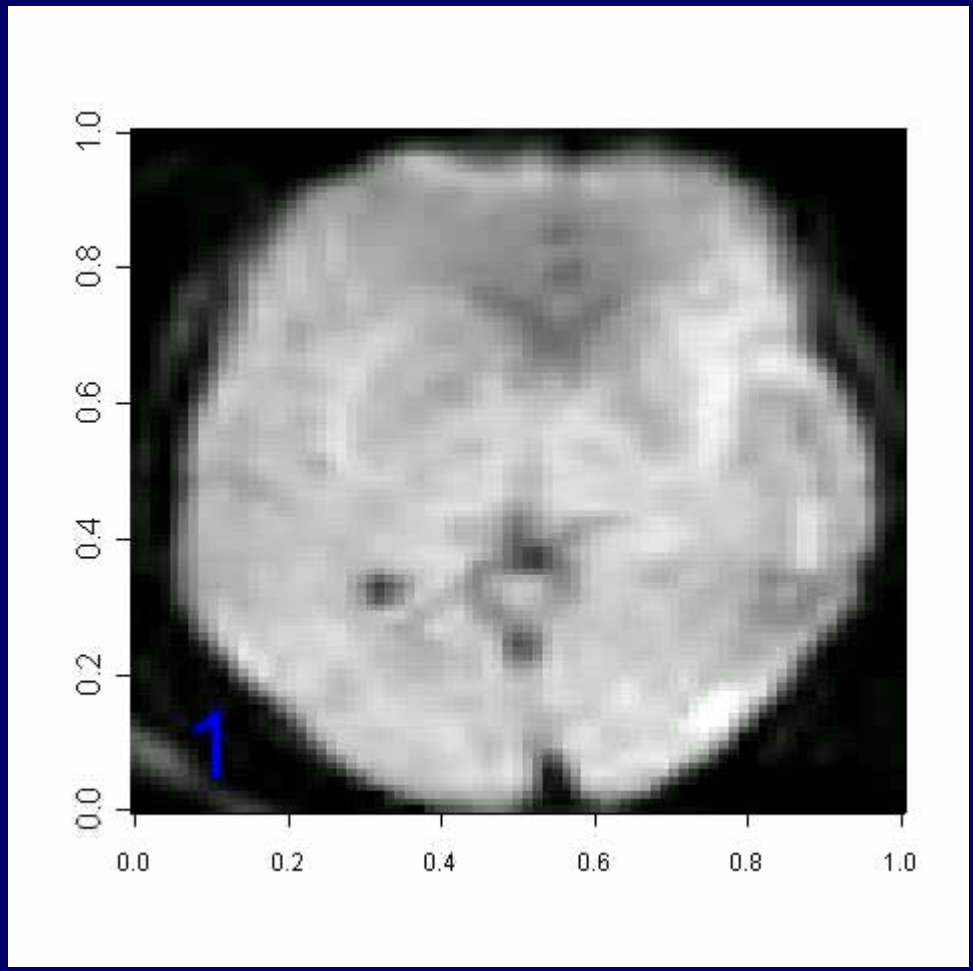

Two stage model

- Approximates random effect analysis by:
  1. Using a multivariate regression model on the bold signal to the hrf convolved design matrix
  2. Slowly varying trend terms serve as a high pass filter
  3. Coefficient maps from this first fitting are then compared across subjects (recall subjects have all been normalized to a template).

Alzheimer's disease

- Degenerative neurological disorder affecting over 2 million Americans above the age of 60 (Brookmeyer et al. 1998)
- Progressive loss of memory, reasoning and language
- No prevention or effective treatment
- Current data suggests pathologic neurological changes occur well before the onset of symptoms
- Increasing age and familiar risk are the best predictors of incident AD
- fMRI may be able to pick up neurological changes in pre-clinical subjects

Alzheimer's disease fMRI study

- Roughly 200 individuals without clinical AD
  - Around 100 at high risk with at least one (autopsy confirmed) affected parent and one first degree relative with a clinical diagnosis of AD
  - Around 100 controls
- Structural and functional images taken at two time points
- Functional images restricted to a narrow band focused around the MTL

FMRI image locations

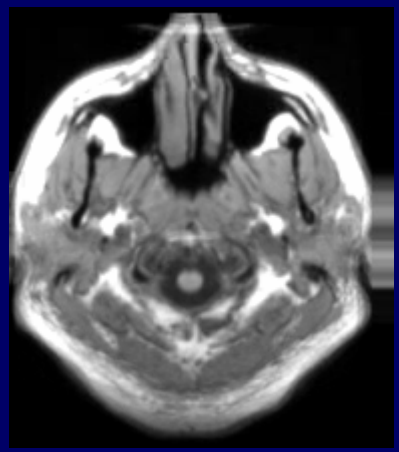

Verbal paired associates paradigm

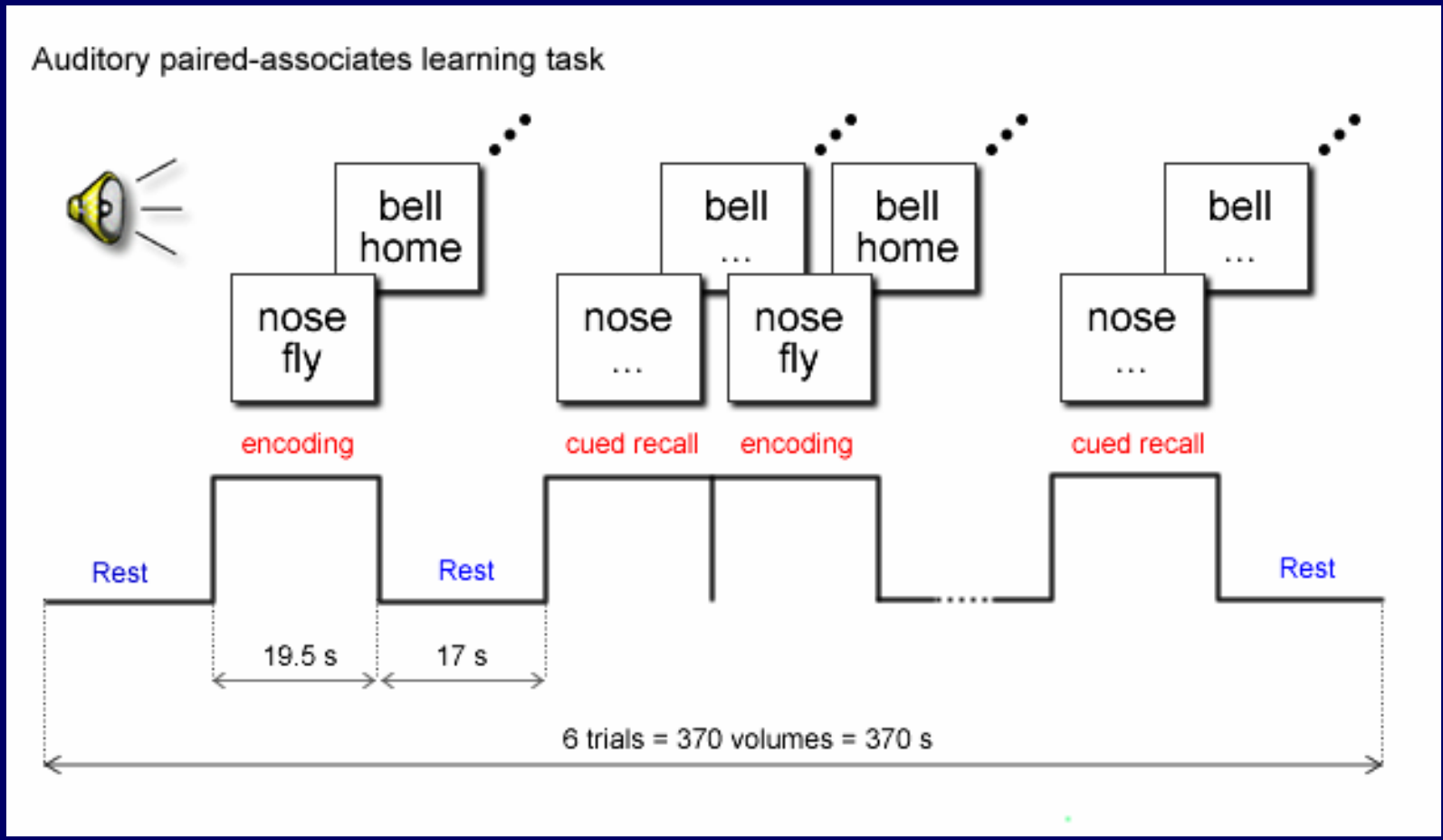

Demographics

Variable	At-Risk (N=95) Mean (sd)	Control (N=90) Mean (sd)
Age	62.01 (6.77)	62.68 (7.88)
Education	15.31 (3.37)	16.10 (3.17)
Gender	M=42% F=58%	M=54% F=46%
Handedness	Right=89% Left=11%	Right=83% Left=17%
# APOE ε4 alleles	0=61% 1= 31% 2=8%	0= 78% 1=20% 2=2%
Paired Associates Test Pre-scanning	12.43 (3.2)	12.19 (3.04)
Paired Associates Test During-fMRI	5.72 (3.64)	5.80 (3.76)

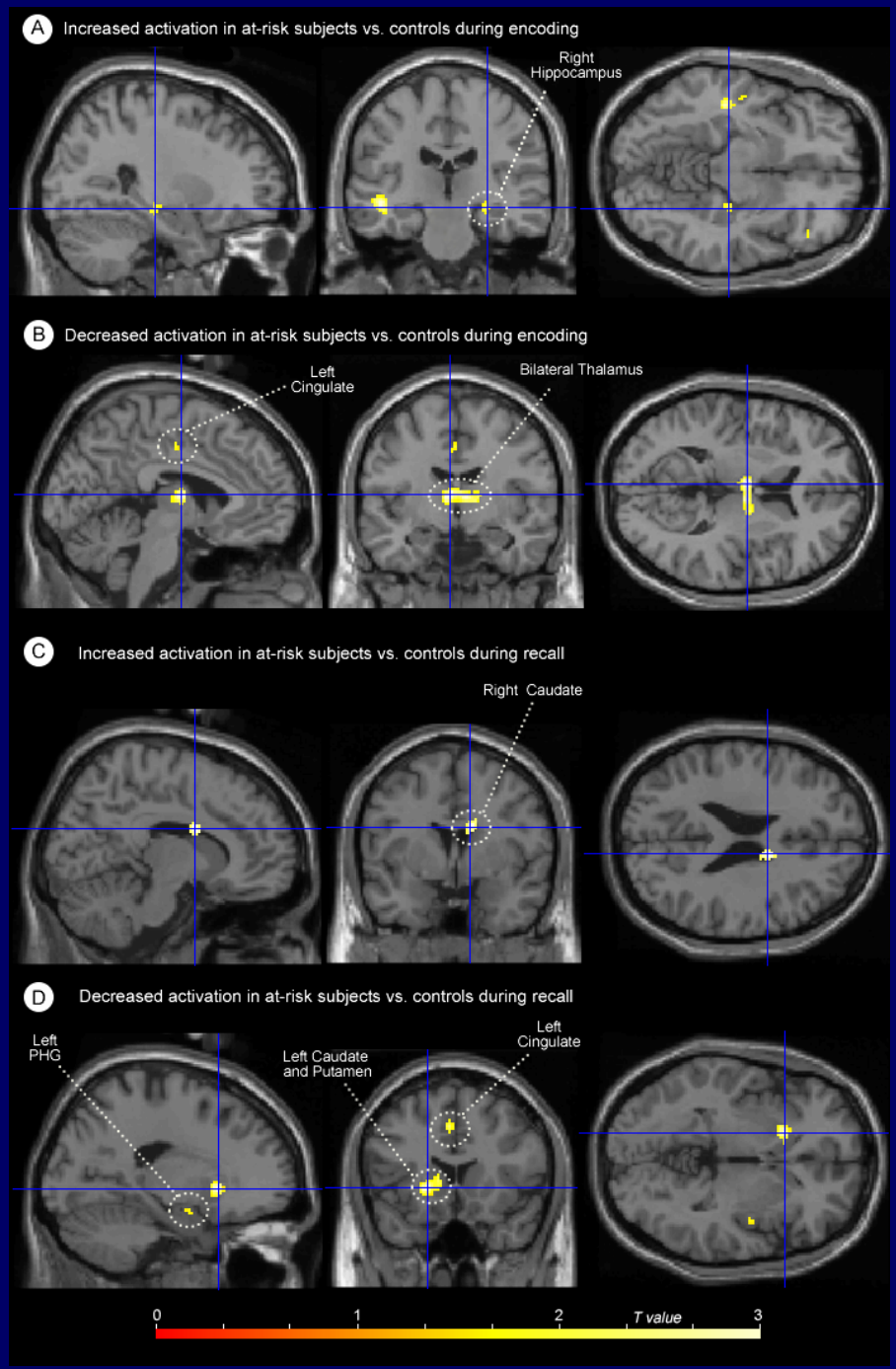
A Increased activation in at-risk subjects vs. controls during encoding
Right Hippocampus
B Decreased activation in at-risk subjects vs. controls during encoding
Left Cingulate
Bilateral Thalamus
C Increased activation in at-risk subjects vs. controls during recall
Right Caudate
D Decreased activation in at-risk subjects vs. controls during recall
Left PHG
Left Caudate and Putamen
Left Cingulate
0
1
2
T value
3

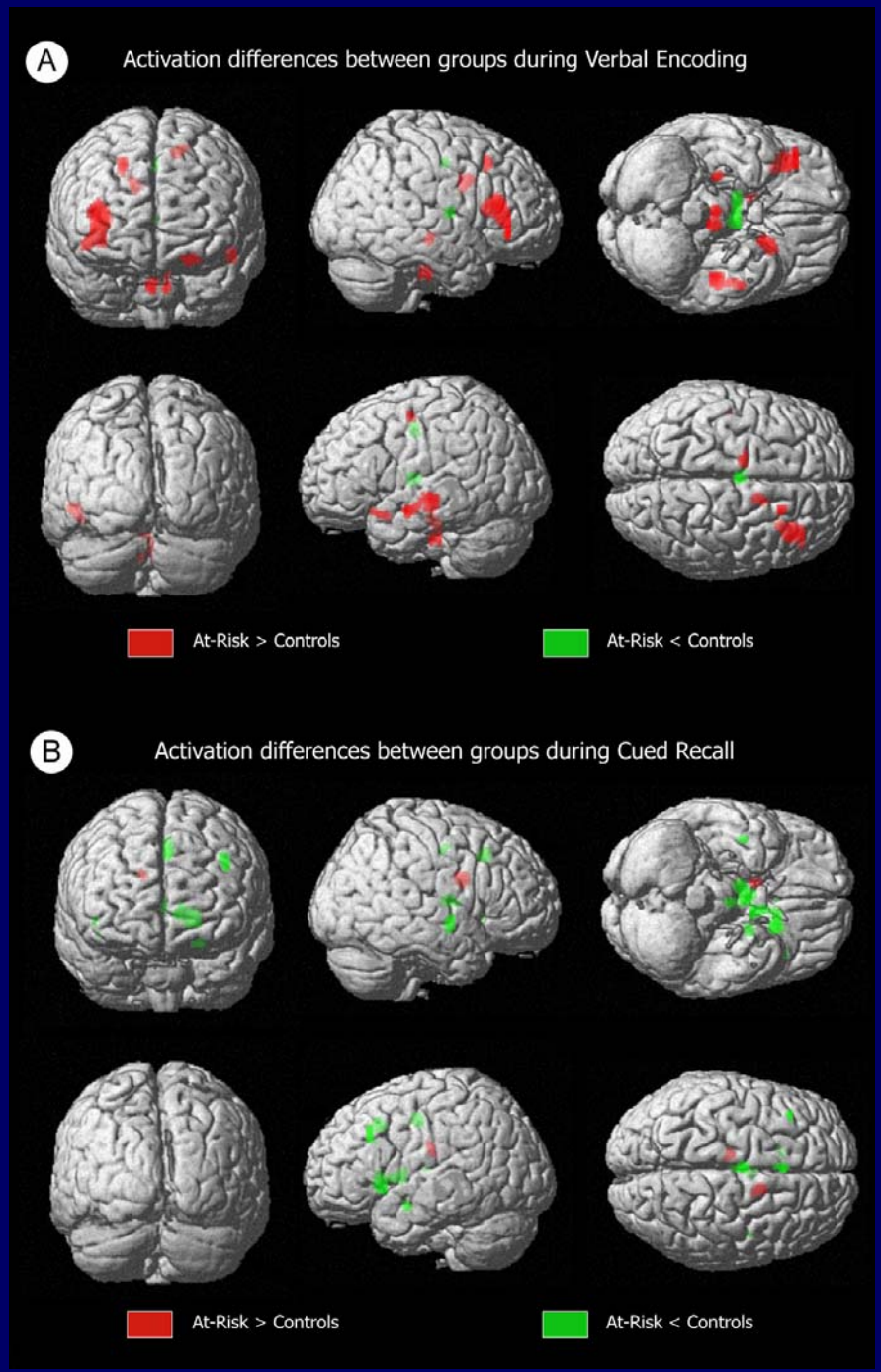
A Activation differences between groups during Verbal Encoding
At-Risk > Controls
At-Risk < Controls
B Activation differences between groups during Cued Recall
At-Risk > Controls
At-Risk < Controls

Methods goal for the Wave II data

- Utilize information from anatomically defined regions / combine voxel-wise and region of interest analyses
- Consider functional connectivity as well as activation
  - Connectivity within regions of interest
  - Connectivity between regions
  - Explore at-risk/control differences in connectivity

ROI creation

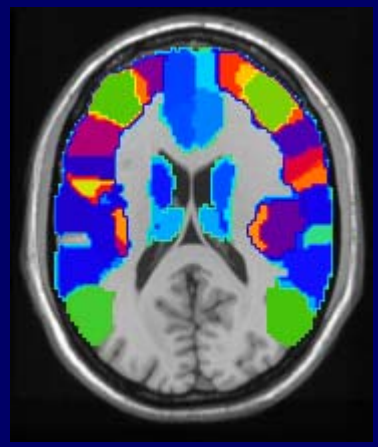

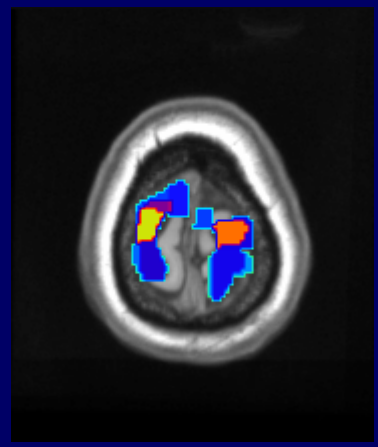

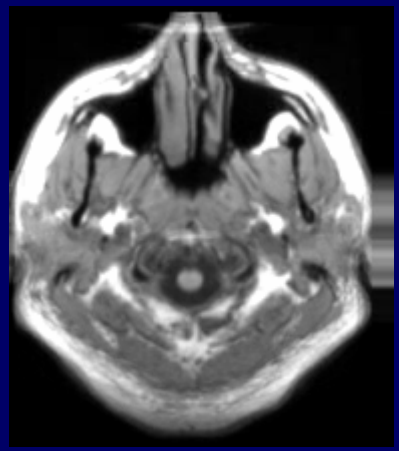

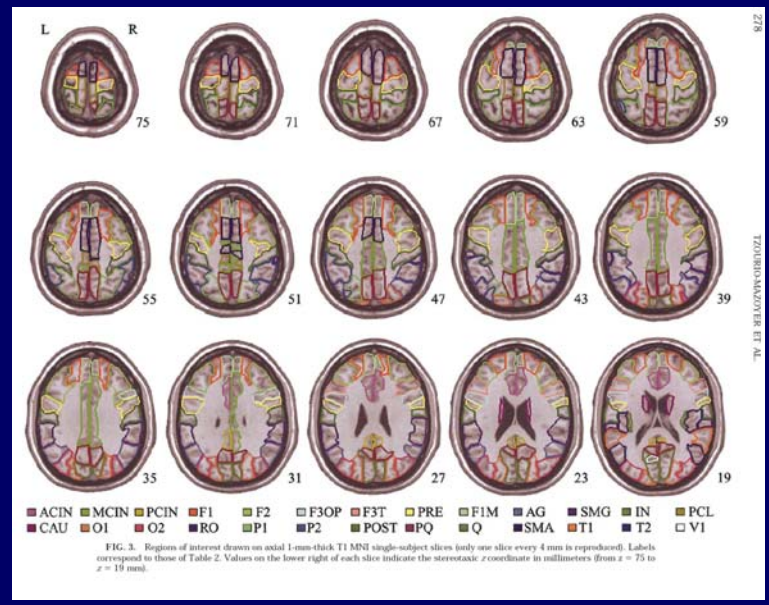

Tzourio-Mazoyer et al. Neuroimage 15

Data preprocessing

- Images are skull stripped timed with the paradigm
- Motion corrected
- Normalized to a standard template (MNI)
- ***Not smoothed***
- Voxel time series regressed on hrf convolved design matrix
- Coefficient maps were retained for second level analysis

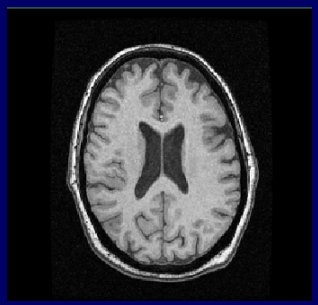
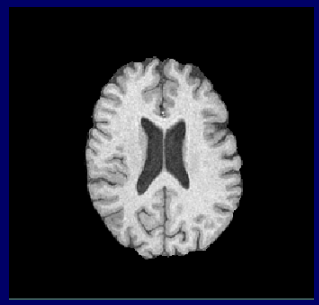
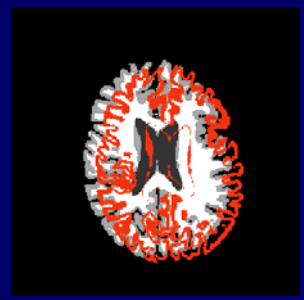
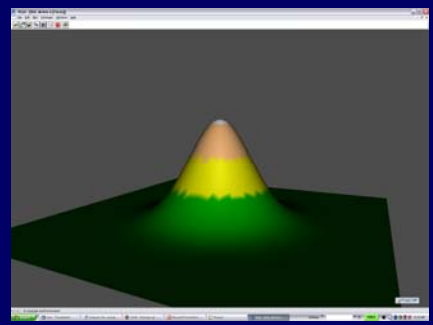

Bayesian analysis of the Wave II data

- Consider the coefficient maps from a first stage analysis
- Posits a hierarchical model that
  - Separate voxel-specific mean for each voxel
  - Assumes an exchangeable correlation for voxels within the same region
  - Assumes an unstructured correlation matrix between regions
- Consider encode versus rest

Data representation

Subject 1

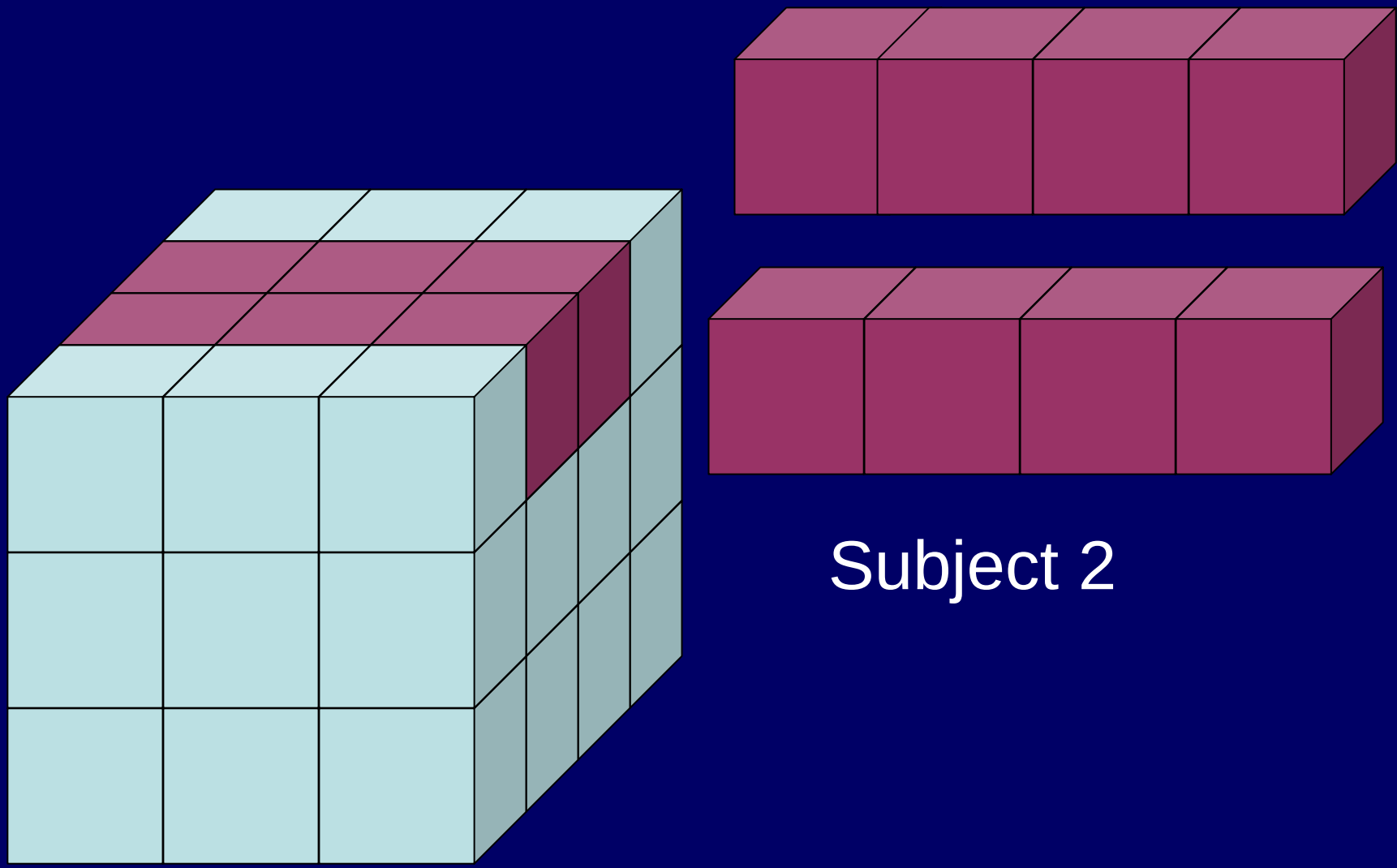

Subject 2

Statistical model

$$
\begin{aligned}
\boldsymbol{\beta}_{igj} \mid \boldsymbol{\mu}_{gj}, \alpha_{igj}, \sigma_{gj}^{-2} &\sim \text{Normal}(\boldsymbol{\mu}_{gj} + \mathbf{1}\alpha_{igj}, \sigma_{gj}^2 \mathbf{I}) \\
\boldsymbol{\mu}_{gj} \mid \lambda_{gj}^2 &\sim \text{Normal}(\boldsymbol{\mu}_{0gj}, \lambda_{gj}^2 \mathbf{I}) \\
\sigma_{gj}^2 \mid \boldsymbol{\Gamma}_j &\sim \text{Gamma}(a_0, b_0) \\
\boldsymbol{\alpha}_{ij} \mid \boldsymbol{\Gamma}_j &\sim \text{Normal}(\mathbf{0}, \boldsymbol{\Gamma}_j) \\
\lambda_{gj}^{-2} &\sim \text{Gamma}(c_0, d_0) \\
\boldsymbol{\Gamma}_j^{-1} &\sim \text{Wishart}\left\{(h_0 \mathbf{H}_{0j})^{-1}, h_0\right\}
\end{aligned}
$$

Statistical model

Voxel- and subject-specific data

Regional and group mean

Subject- and region-specific random itc

$$
\begin{aligned}
\boldsymbol{\beta}_{igj} \mid \boldsymbol{\mu}_{gj}, \alpha_{igj}, \sigma_{gj}^{-2} &\sim \text{Normal}(\boldsymbol{\mu}_{gj} + \mathbf{1}\alpha_{igj}, \sigma_{gj}^2 \mathbf{I}) \\
\boldsymbol{\mu}_{gj} \mid \lambda_{gj}^2 &\sim \text{Normal}(\boldsymbol{\mu}_{0gj}, \lambda_{gj}^2 \mathbf{I}) \\
\sigma_{gj}^2 \mid \boldsymbol{\Gamma}_j &\sim \text{Gamma}(a_0, b_0) \\
\boldsymbol{\alpha}_{ij} \mid \boldsymbol{\Gamma}_j &\sim \text{Normal}(\mathbf{0}, \boldsymbol{\Gamma}_j) \\
\lambda_{gj}^{-2} &\sim \text{Gamma}(c_0, d_0) \\
\boldsymbol{\Gamma}_j^{-1} &\sim \text{Wishart}\left\{(h_0 \mathbf{H}_{0j})^{-1}, h_0\right\}
\end{aligned}
$$

Between-region correlation matrix

Discussion

- The AD data set is well suited to such an analysis
  - Large number of subjects per group
  - Relatively small coronal band considered
    - Allows for a finer decomposition of ROIs

Full conditionals

$$
\begin{aligned}
\boldsymbol{\mu}_{gj} &\sim \text{Normal}\left[\boldsymbol{\Omega}_{gj}\left\{\lambda_{gj}^{-2}\mu_{0gj} + K_j\sigma_{gj}^{-2}(\bar{\boldsymbol{\beta}}_{gj} - \mathbf{1}\bar{\boldsymbol{\alpha}}_{gj})\right\}, \boldsymbol{\Omega}_{gj}\right] \\
\sigma_{gj}^{-2} &\sim \text{Gamma}\left\{\alpha_0 + K_j V_g/2, \left(\frac{1}{b_0} + \frac{1}{2}\sum_{i=1}^{K_j} u_{igj}\right)^{-1}\right\} \\
\boldsymbol{\alpha}_{ij} &\sim \text{Normal}\left[\boldsymbol{\psi}_j\left\{\mathbf{D}_j^{-1}(\bar{\boldsymbol{\beta}}_{ij} - \bar{\boldsymbol{\mu}}_j)\right\}, \boldsymbol{\psi}_j\right] \\
\lambda_{gj}^{-2} &\sim \text{Gamma}\left\{c_0 + V_g/2, \left(\frac{1}{d_0} + \frac{(\boldsymbol{\mu}_{gj} - \boldsymbol{\mu}_{0gj})'(\boldsymbol{\mu}_{gj} - \boldsymbol{\mu}_{0gj})}{2}\right)^{-1}\right\} \\
\boldsymbol{\Gamma}_j^{-1} &\sim \text{Wishart}\left\{\left(h_0\mathbf{H}_0 + \sum_{i=1}^{K_j}\boldsymbol{\alpha}_{ij}\boldsymbol{\alpha}_{ij}'\right)^{-1}, h_0 + K_j\right\},
\end{aligned}
$$

Intra-regional connectivity

- Exchangeable covariance structure for voxels within a region

$$\mathrm{Var}(\boldsymbol{\beta}_{igj} \mid \boldsymbol{\mu}_{gj}) = \gamma_{gg}^{(j)}\mathbf{J} + \sigma_{gj}^2\mathbf{I},$$

- Measure of intra-regional connectivity

$$\rho_{gj} = \frac{\gamma_{gg}^{(j)}}{\gamma_{gg}^{(j)} + \sigma_{gj}^2}.$$

Inter-regional connectivity

- The unstructured variance matrix between regions represents inter-regional connectivity

$$\{\mathrm{Diag}(\mathbf{\Gamma}_j)\}^{-1/2}\,\mathbf{\Gamma}_j\,\{\mathrm{Diag}(\mathbf{\Gamma}_j)\}^{-1/2}$$

- Requires several subjects depending on how small the regions are

Running the chain

- Chains were started at moment based estimates
- Run for 10,000 iterations
- Subsampled the chain to retain whole brain information (though used all simulations for posterior mean estimates)
- Used batch means to estimate MC standard errors
- Varied the hyperparameter values to evaluate robustness of conclusions to assumptions

Voxel-level results

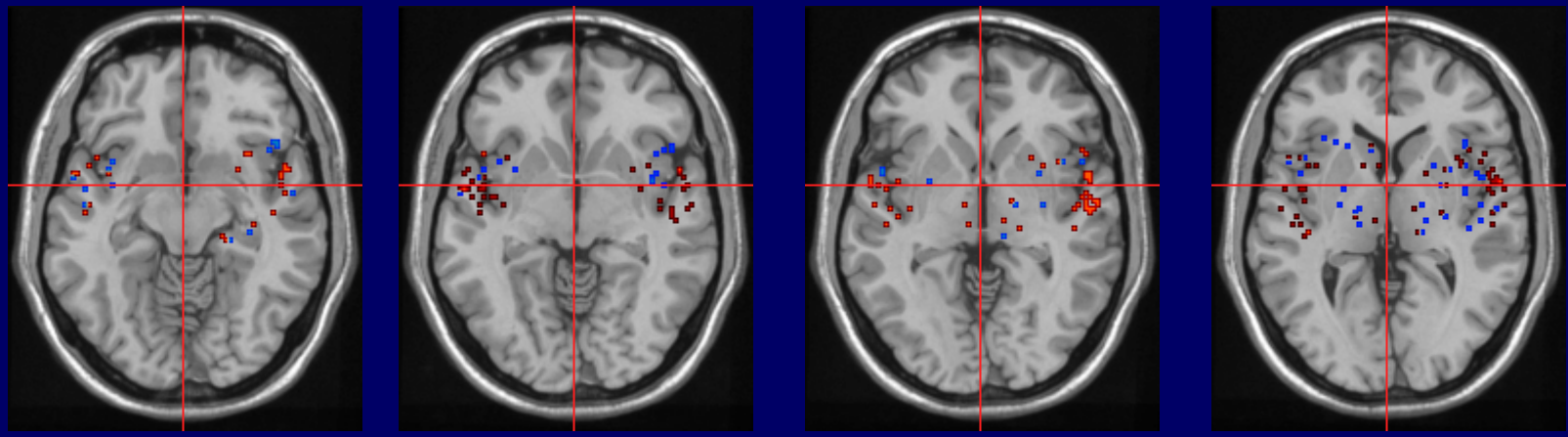

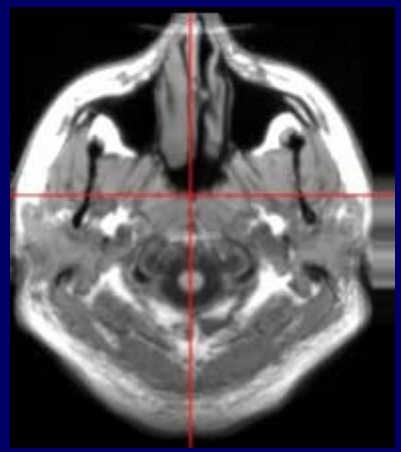

ROI results

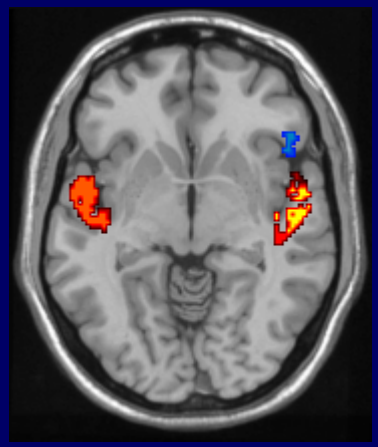
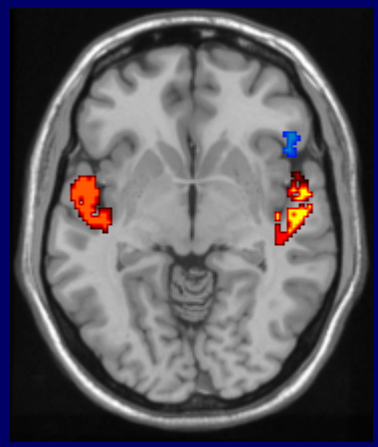
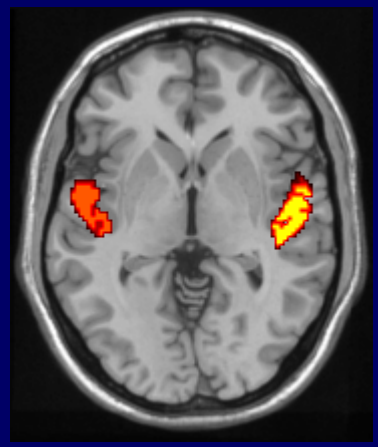
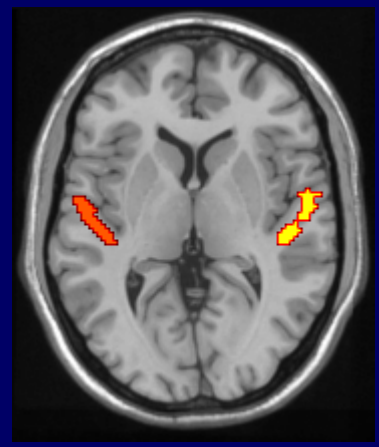
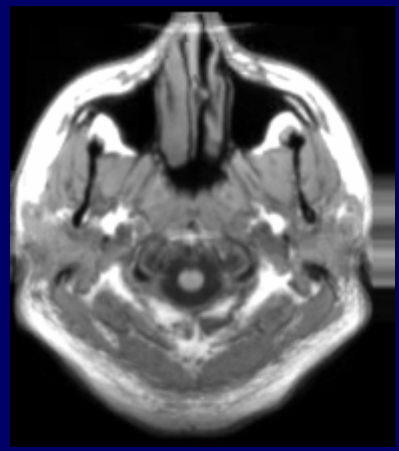

Inta-regional posterior mean connectivity estimates

Region	**Ctr**	**AR**	**CI**
L A Cing	0.18	0.26	[0.52, 0.92]
R A Cing	0.16	0.26	[0.47, 0.84]
L Mid Cing	0.16	0.22	[0.53, 0.98]
R Inf Tr FR	0.18	0.26	[0.54, 0.96]
L Sup Fr	0.23	0.33	[0.54, 0.92]

Posterior mean functional connectivity matrix, controls

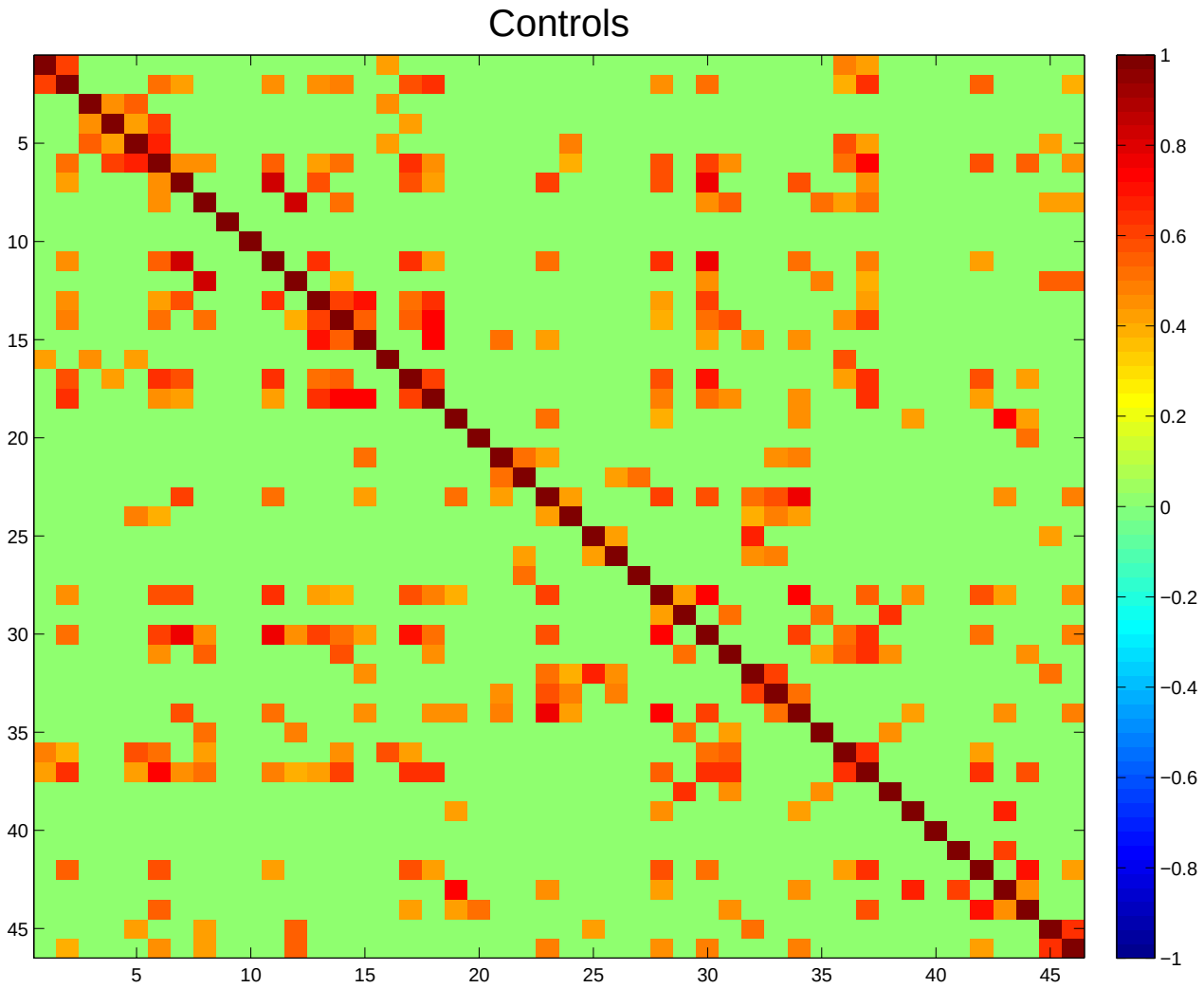

Posterior mean functional connectivity matrix, at-risk

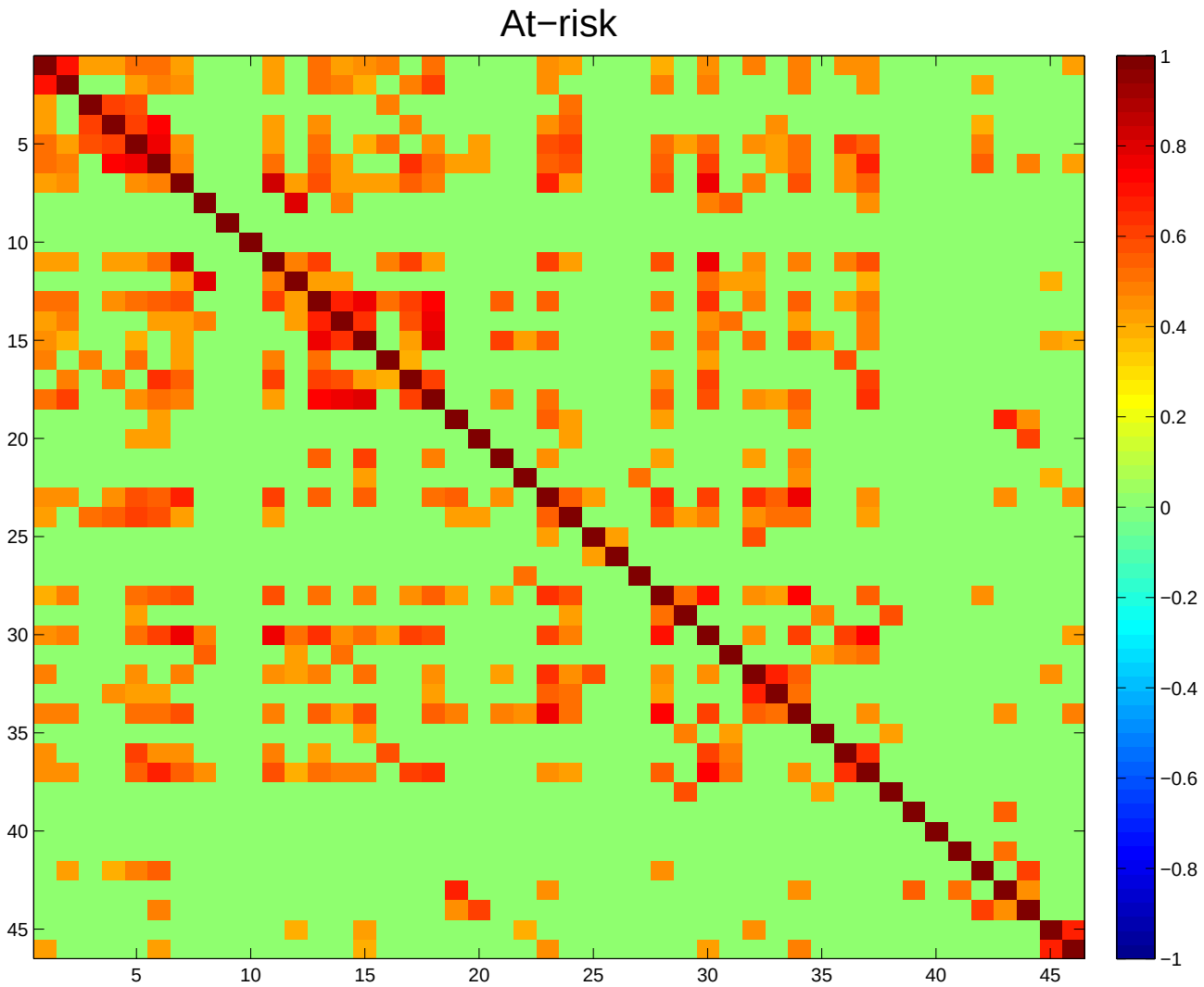

Functional connectivity results

- Ratio of determinants had a credible interval of [1.08, 109.95]
- Greatest root statistic (Mardia et al. 1979) had a credible interval of [.87, .91]

Summary of results

- No relevant voxel level activations in the second wave
  - potentially due to the relatively fine decomposition into regions of interest
- Regional mean activations show mild evidence of group differences
- Interesting group differences in intra-regional functional connectivity
- Interesting group differences in inter-regional functional connectivity

Extensions

- Longitudinal data
- Better priors on the covariance matrices
- Consider encode / recall data simultaneously
- Retain some of the temporal information from the first stage

- Exploration of connectivity for the wave I data
- Non-anatomically derived regions

Acknowledgements

- DuBois Bowman
- Susan Bassett
- Clinton Kilts